

The effects of apolipoprotein B depletion on HDL subspecies composition and function^S

W. Sean Davidson,* Anna Heink,[†] Hannah Sexmith,[†] John T. Melchior,* Scott M. Gordon,[§] Zsuzsanna Kuklenyik,** Laura Woollett,* John R. Barr,** Jeffrey I. Jones,** Christopher A. Toth,^{††} and Amy S. Shah^{1,†}

Center for Lipid and Arteriosclerosis Science,* Department of Pathology and Laboratory Medicine, University of Cincinnati, Cincinnati, OH 45237; Department of Pediatrics,[†] Cincinnati Children's Hospital Research Foundation, Cincinnati, OH 45229; National Heart, Lung, and Blood Institute,[§] Lipoprotein Metabolism Section, Bethesda, MD 20892; Division of Laboratory Sciences,** National Center for Environmental Health, Centers for Disease Control and Prevention, Atlanta, GA 30341; and Battelle Memorial Institute,^{††} Analytical Services, Atlanta, GA 30329

Abstract HDL cholesterol (HDL-C) efflux function may be a more robust biomarker of coronary artery disease risk than HDL-C. To study HDL function, apoB-containing lipoproteins are precipitated from serum. Whether apoB precipitation affects HDL subspecies composition and function has not been thoroughly investigated. We studied the effects of four common apoB precipitation methods [polyethylene glycol (PEG), dextran sulfate/magnesium chloride (MgCl₂), heparin sodium/manganese chloride (MnCl₂), and LipoSep immunoprecipitation (IP)] on HDL subspecies composition, apolipoproteins, and function (cholesterol efflux and reduction of LDL oxidation). PEG dramatically shifted the size distribution of HDL and apolipoproteins (assessed by two independent methods), while leaving substantial amounts of reagent in the sample. PEG also changed the distribution of cholesterol efflux and LDL oxidation across size fractions, but not overall efflux across the HDL range. Dextran sulfate/MgCl₂, heparin sodium/MnCl₂, and LipoSep IP did not change the size distribution of HDL subspecies, but altered the quantity of a subset of apolipoproteins. Thus, each of the apoB precipitation methods affected HDL composition and/or size distribution. **EW** We conclude that careful evaluation is needed when selecting apoB depletion methods for existing and future bioassays of HDL function.—Davidson, W. S., A. Heink, H. Sexmith, J. T. Melchior, S. M. Gordon, Z. Kuklenyik, L. Woollett, J. R. Barr, J. I. Jones, C. A. Toth, and A. S. Shah. **The effects of apolipoprotein B depletion on HDL subspecies composition and function.** *J. Lipid Res.* 2016. 57: 674–686.

Supplementary key words polyethylene glycol • dextran sulfate • heparin sodium • lipoproteins • high density lipoprotein • low density lipoprotein • proteomics • cholesterol efflux

This work was supported by National Heart, Lung, and Blood Institute Grants R01HL67093 (W.S.D.), R01HL104136 (W.S.D.), and K23HL118132 (A.S.S.). The authors declare no financial conflicts of interest relevant to this study. The content is solely the responsibility of the authors and does not necessarily represent the official views of the National Institutes of Health.

Manuscript received 16 January 2016 and in revised form 17 February 2016.

Published, JLR Papers in Press, February 23, 2016
DOI 10.1194/jlr.M066613

Epidemiological studies show a strong inverse relationship between circulating levels of HDL cholesterol (HDL-C) and coronary artery disease (CAD) in patients with high, normal, or low LDL cholesterol (LDL-C) levels (1, 2). However, HDL-C-raising therapies using cholesteryl ester transfer protein (CETP) inhibitors have not been fruitful with respect to protection from CAD, despite raising HDL-C levels significantly. Additionally, Mendelian randomization studies have revealed that genetic mutations that specifically raise HDL-C do not necessarily confer CAD benefits (3–6). Thus, HDL-C may not be an appropriate biomarker for CAD risk, particularly given new information about the proteomic and lipidomic complexity underlying HDL particles (7–9).

Recently, attention has shifted to HDL function as a potential biomarker for CAD risk. The function most commonly associated with HDL is its ability to mobilize or “efflux” cholesterol from cells in the periphery and transport it to the liver for catabolism (10). It is widely believed that HDL-mediated removal of cholesterol from enriched cells in the vessel wall, particularly macrophages, is a key reason for its association with CAD protection. Indeed, many studies have shown that HDL particles isolated by ultracentrifugation from diseased individuals versus normal controls are defective in efflux capacity (11–13).

However, HDL isolation by ultracentrifugation is a lengthy procedure that likely disrupts HDL particles (14),

Abbreviations: AF4, asymmetric flow field-flow fractionation; AUC, area under the curve; CAD, coronary artery disease; HDL-C, HDL cholesterol; IP, immunoprecipitation; LDL-C, LDL cholesterol; MgCl₂, magnesium chloride; MnCl₂, manganese chloride; MW, molecular weight; PEG, polyethylene glycol; STB, standard Tris buffer.

To whom correspondence should be addressed.

e-mail: amy.shah@cchmc.org

^S The online version of this article (available at <http://www.jlr.org>) contains a supplement.

making this approach problematic for large scale clinical studies. As a result, clinical studies have begun to evaluate HDL function in situ by precipitating the apoB-containing lipoproteins (LDL and VLDL) out of plasma or serum in order to remove their background activities.

In a landmark study, Khera et al. (15) found that cholesterol efflux capacity from cultured macrophages (after apoB precipitation) was strongly and inversely associated with both subclinical atherosclerosis (measured by carotid artery intima-media thickness) and angiographically confirmed obstructive CAD. The efflux capacity outperformed measures of total cholesterol, LDL-C, and HDL-C with respect to the odds ratios for CAD. Then Rohatgi et al. (16) prospectively confirmed this association in a large population that was free of disease at baseline. For a review of the studies evaluating cholesterol efflux in human disease, see (17).

A popular reagent used to precipitate LDL and VLDL out of serum is polyethylene glycol (PEG) (15, 16). PEG is a neutral polymer that reduces the solubility of LDL and VLDL (18). Other methods for apoB precipitation include combining polyvalent anions, like heparin and dextran sulfate, with a divalent cation, such as manganese or magnesium. The polyanions interact with arginine and other positively charged residues on apolipoproteins, while the cations help the polyanion-lipoprotein complexes form via interaction with phospholipids resulting in precipitation. Dextran sulfate-magnesium chloride (MgCl_2) is the most widely used method to quantify HDL-C in most clinical laboratories (19). In strict terms, none of these methods have “specificity” for LDL or VLDL on a molecular basis, such as seen with immunoprecipitations. These reagents are titrated into plasma or serum to an extent that their actions have a disproportionate impact on large apoB-containing lipoproteins versus smaller HDL particles.

Upon their introduction, each apoB precipitation method was carefully optimized and verified to quantitatively deplete LDL-C with minimal impact on HDL-C. For example, in the mid-1980s, methods of apoB depletion on HDL-C quantification and apoA-I levels were compared (20, 21). However, we and others have shown that HDL is composed of a heterogeneous population of particles with diversity in their proteomic fingerprint (7, 9, 22, 23) and physical properties [solubility, size (24), and ability to interact with proteoglycans (25)]. These recent advances in our understanding of HDL diversity require a reassessment of the impact of apoB lipoprotein depletion methods on HDL subspecies composition and function. This is important because artifactual alterations in HDL subspecies levels or composition could have profound impact not only on downstream functional measurements, like cholesterol efflux, but also on other HDL functions, including anti-inflammation and protection of LDL from oxidation.

Here, we assessed the impact of the three most widely used apoB lipoprotein depletion methodologies on HDL subspecies profiles, apolipoprotein content, and HDL function in terms of cholesterol efflux and ability to protect

LDL from oxidation. We also tested a proprietary immunoprecipitation (IP) reagent prepared from delipidated goat anti-apoB serum that binds and removes apoB-containing lipoproteins. We found that there is no perfect method with respect to the impact on the HDL-sized species in terms of size, protein content, and function.

MATERIALS AND METHODS

Blood collection

Three healthy nonsmoking normolipidemic females with a mean age of 28.7 years were studied. Fasting blood was collected in a red top serum separator (Becton Dickinson Biosciences), allowed to clot for 30 min at room temperature, and then spun at $\sim 1,590 g$ for 15 min to isolate serum. These studies were approved by the Institutional Review Board at Cincinnati Children’s Hospital Medical Center and informed consent was obtained.

Gel filtration chromatography

After collection, 370 μl of serum was applied to three Superdex 200 Increase columns arranged in series (10/300; GE Healthcare), as previously described (23). Samples were eluted in 10 mM Tris and 0.15 M NaCl at pH 8.2, hereafter referred to as standard Tris buffer (STB). The eluate was collected as 47 fractions (fraction collector F9-C; GE Healthcare) of 1.5 ml maintained at 4°C. To relate gel filtration results to traditional density-centric definitions, we used the presence of apoB, the core constituent of LDL and VLDL, as a distinguisher (23). Therefore, the VLDL/LDL range is defined as fractions 15–19 due to the presence of apoB. We assigned the remaining fractions 20–29 as the HDL range, because their diameters range from about 15 to 7 nm in diameter, consistent with measurements for density-isolated HDL and due to the abundance of the major HDL protein, apoA-I (23). See supplementary Fig. 1 for these details. Choline-containing phospholipid and total cholesterol were measured in each fraction using colorimetric kits from Wako (Richmond, VA) and Pointe Scientific (Canton, MI), respectively. Serum was stored at 4°C between experiments and was never frozen.

apoB depletion methods

To remove apoB-containing lipoproteins from fasted serum, the following methods were employed: 1) PEG [molecular weight (MW) 6,000; Sigma-Aldrich, St. Louis, MO] precipitation. PEG (400 μl) (20% in water) was added to 1 ml serum, incubated for 20 min at room temperature, and then centrifuged at 10,000 rpm for 30 min. 2) Dextran sulfate/ MgCl_2 (Sigma-Aldrich) precipitation. Dextran sulfate (20 μl) (5% in water) and 25 μl of 2 M MgCl_2 were added to 1 ml serum, incubated for 20 min at room temperature, and then centrifuged at 3,000 g for 10 min (26). 3) Heparin sodium/manganese chloride (MnCl_2 ; Sigma-Aldrich) precipitation. Heparin sodium (40 μl) (1.3 mg/ml in 150 mM saline) and 50 μl of 1 M MnCl_2 added to 1 ml serum, incubated for 30 min at 4°C, and then centrifuged at 1,500 g for 30 min (27). 4) LipoSep IP (Sun Diagnostics, New Gloucester, ME). LipoSep IP is a proprietary IP reagent prepared from delipidated goat anti-apoB antisera. LipoSep IP reagent (1 ml) was added to an equal volume (1 ml) of serum, incubated for 10 min at room temperature, and then centrifuged at 12,000 rpm for 10 min (per the suggested manufacturer’s recommendations).

For each method, the pellet (containing apoB lipoproteins) was discarded and the remaining supernatant (containing HDL) was applied to the Superdex 200 Increase columns as above. To

account for dilution effects of these reagents, prior to use, all apoB depleted samples and control serum were diluted with STB to equal volumes of 1.4 ml (or 2 ml for comparisons using Liposep IP reagent).

Western blot

Confirmation of complete apoB depletion from serum samples was performed via a Western blot for apoB. Serum, apoB-depleted serum from each method, and an ultracentrifugally isolated LDL control (75 ng protein) were resolved by SDS-PAGE (4–15%) and transferred to a polyvinylidene difluoride membrane. The membrane was blotted with goat anti-human apoB diluted 1:2,500 (K45253G; Meridian Life Sciences, Memphis, TN) and detected using donkey anti-goat IgG-HRP diluted 1:2,500 (SC2056; Santa Cruz, Dallas, TX).

apoA-I immunoblotting was performed on serum and apoB-depleted serum fractions in the HDL subspecies range (fractions 20–30). Ten microliters of each fraction was resolved by SDS-PAGE (4–15%) and transferred to a polyvinylidene difluoride membrane. The membrane was blotted with rabbit anti-human apoA-I diluted 1:2,500 (178422; EMD Millipore) and detected using donkey anti-rabbit IgG-HRP diluted 1:2,500 (NA934V; GE Healthcare). Densitometry analysis was performed using ImageJ (National Institutes of Health).

Immunodot blot

Immunodot blotting for the detection of apoE in HDL-range fractions (fractions 20–26) from serum and apoB-depleted serum was carried out using a Bio-Dot apparatus (Bio-Rad, Hercules, CA). Thirty-five microliters of each fraction was transferred onto a nitrocellulose membrane in 300 μ l Tris-buffered saline [20 mM Tris, 150 mM NaCl (pH 7.6)]. The membrane was blocked with Odyssey PBS blocking buffer (LiCor Biosciences, Lincoln, NE) and blotted with mouse anti-human apoE diluted 1:1,200 (SC53570; Santa Cruz). Detection was performed using goat anti-mouse IgG-Alexa Fluor 680 conjugate diluted 1:40,000 (A21058; Life Technologies) in Odyssey blocking buffer containing 0.01% SDS. The membrane was imaged using an Odyssey infrared imaging system (LiCor Biosciences). Densitometry analyses were accomplished using the Odyssey application software, version 2.0.41.

HDL function

Cholesterol efflux was assessed as the movement of ^3H -labeled cholesterol from RAW 264.7 macrophages, a murine macrophage cell line (ATCC, Manassas, VA), to the medium containing fractionated serum samples. Cultured cells were plated in 48-well plates. The following day, cells were incubated overnight with labeling medium (high-glucose DMEM with 10% fetal bovine serum and 1% penicillin-streptomycin) containing 1 $\mu\text{Ci}/\text{ml}$ of ^3H -cholesterol (PerkinElmer, Boston, MA) and 2 $\mu\text{g}/\text{ml}$ of an ACAT inhibitor (Sandoz 58-035; Sigma-Aldrich). The 8-Br-cAMP (Sigma-Aldrich) at a final concentration of 0.3 mM was added to all experimental and control wells to induce efflux via ABCA1, ABCG1, and aqueous diffusion (28, 29). The next day, treatments containing 33.3% v/v of each serum fraction or apoB-depleted serum fraction were freshly made in basal medium (consisting of DMEM containing 0.2% BSA). It should be noted that each serum fraction was approximately 50-fold dilute compared with serum. Control treatments containing lipid-free apoA-I and HDL (each at 10 $\mu\text{g}/\text{ml}$ protein) with and without 8-Br-cAMP were also made. Labeling medium was removed from the cells, and each well was washed twice with PBS. One hundred and fifty microliters of each treatment were added per well and incubated for 6 h. In order to measure the

mean amount of ^3H -cholesterol present inside the cells at the time of treatment addition, ^3H -cholesterol was extracted from radiolabeled cells on a separate T0 plate by washing the wells with isopropanol, drying down the isopropanol wash, and then resuspending the dried extract in 150 μl toluene. Following incubation, treatment medium was then collected, filtered through a 0.45 μm 96-well filter plate, and measured for detection of ^3H -cholesterol effluxed to acceptor via scintillation counting. Percent cholesterol efflux is expressed using the following formula: ^3H count in efflux media / (^3H count in efflux media + mean ^3H count extracted from untreated cells) \times 100. All experimental and control samples were assayed in triplicate.

Anti-oxidative activity of apoB-depleted serum was assessed toward an exogenous reference ultracentrifugally-isolated LDL sample using the method of Kontush, Chantepie, and Chapman (30). LDL was stored at -80°C with 6.25% sucrose (w/v). In a UV transparent 96-well microplate, 20 μg LDL-C per well was combined with 65 μl of serum or apoB-depleted serum fraction and brought up to 200 μl with STB. After incubating the plate for 10 min at 37°C , 100 mM 2,2'-azobis(2-methylpropanamide) dihydrochloride was added to each well at a final concentration of 5 mM to initiate LDL oxidation. Conjugated diene absorbance at 234 nm was read every 5 min for 8 h at 37°C . The kinetic curves generated for each sample were analyzed to calculate the maximum rate of the propagation phase (V_{max}). All data were then normalized to control LDL (not containing any treatment) by dividing the maximal rate of propagation of the sample by the maximal rate of propagation of the LDL control condition, and expressing this value as a percentage. In this assay, protective HDL subspecies decreased the rate of LDL oxidation resulting in a decrease in V_{max} (30).

Asymmetric flow field-flow fractionation

As an alternative method to study the effects of apoB precipitation on lipoprotein subspecies, we used asymmetric flow field-flow fractionation (AF4). This separation technique is based on the fundamental nature of laminar flow. A liquid medium passes through a thin channel, which causes it to adopt a parabolic velocity profile across the height of the channel, with stream velocities faster at the center of the channel and slower near the walls. When serum is injected into this stream, contained particles are subjected to a second perpendicular field created by withdrawal of carrier fluid through a semipermeable membrane that drives them toward the accumulation wall, where they experience slower flow rates. Once they are concentrated at the accumulation wall, particle species begin to diffuse up away from the accumulation wall via Brownian motion into higher velocity flow regimes. Differential retention is caused by the different average height achieved by particles of different sizes, with smaller particles having a higher average height, which results in them eluting faster. The AF4 separation requires no filtration or other sample pretreatment and is achieved by gentle fluid dynamics; both of these elements minimize the risk of introducing artifacts during separation. Serum (50 μl) and 50 μl serum after apoB-depletion with PEG, dextran sulfate/MgCl₂, and heparin sodium/MnCl₂ apoB depletion were injected into an AF2000 system. Samples were analyzed in a buffer solution, prepared of 10 mM sodium bicarbonate and 150 mM NaCl, adjusted to pH 7.4, which was vacuum filtered prior to use. The eluent was collected as 40 fractions of approximately 200 μl maintained at 4°C , starting at 5 min in 2.5 min intervals. Choline-containing phospholipid was measured in each fraction using colorimetric kits from Wako (Richmond, VA). In addition, apolipoprotein analysis was performed via trypsin digestion and

LC-MS/MS. For LC-MS/MS method details, see the supplementary Methods.

Statistics

Data are presented as mean \pm SD. For any analysis where apoB depletion methods were compared with serum, a two-tailed Student's *t*-test was used. *P* < 0.01 was considered significant. A lower threshold was used to decrease the possibility of false positives given the multiple comparisons across the HDL subspecies distribution.

RESULTS

Lipoprotein profiles

The phospholipid and total cholesterol concentrations in control serum across lipoprotein subspecies separated by gel filtration chromatography are shown in black in Fig. 1A, B.

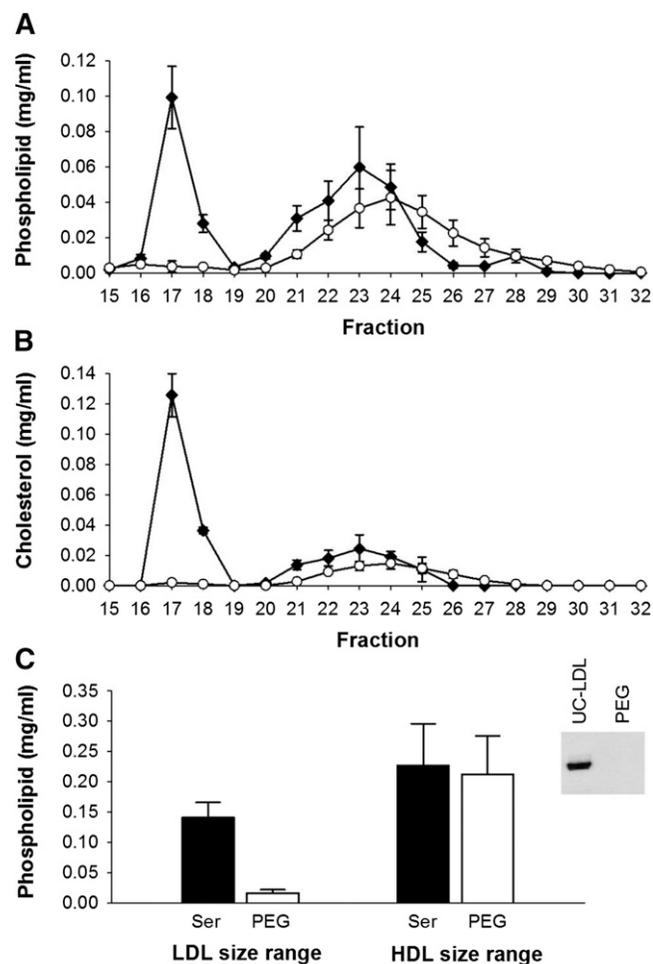


Fig. 1. Phospholipid and cholesterol distribution across lipoprotein subspecies separated by gel filtration chromatography before and after apoB depletion of serum by PEG. Data are mean and SD (*n* = 3). Serum control versus apoB depletion using PEG. All samples were diluted with STB to equal volume prior to gel filtration chromatography. Phospholipid distribution (A), cholesterol distribution (B), and area under the curve (AUC) of LDL and HDL fractions in serum versus apoB-depleted serum (C). The inset in (C) shows Western blot detection of apoB after serum apoB depletion with PEG, demonstrating full precipitation of apoB-containing particles. Serum control (black diamond); PEG apoB-depleted serum (open circle).

LDL and VLDL appeared in a single peak between fractions 15 and 19, while the HDL-sized lipoproteins eluted from large to small in fractions 20–29. The total cholesterol concentration in control serum across lipoprotein subspecies mirrored the phospholipid concentration, except that cholesterol was less prevalent in smaller HDL-sized particles after fraction 26.

When PEG was used to precipitate apoB-containing lipoproteins, the concentration of phospholipid (Fig. 1A) and cholesterol (Fig. 1B) decreased to baseline in fractions 15–19, indicating quantitative removal of these lipoproteins. This was confirmed by the complete disappearance of apoB, shown by the Western blot in Fig. 1C. Interestingly, the HDL-sized lipoproteins underwent a marked rightward shift in their phospholipid and cholesterol profile, implying a change to overall smaller

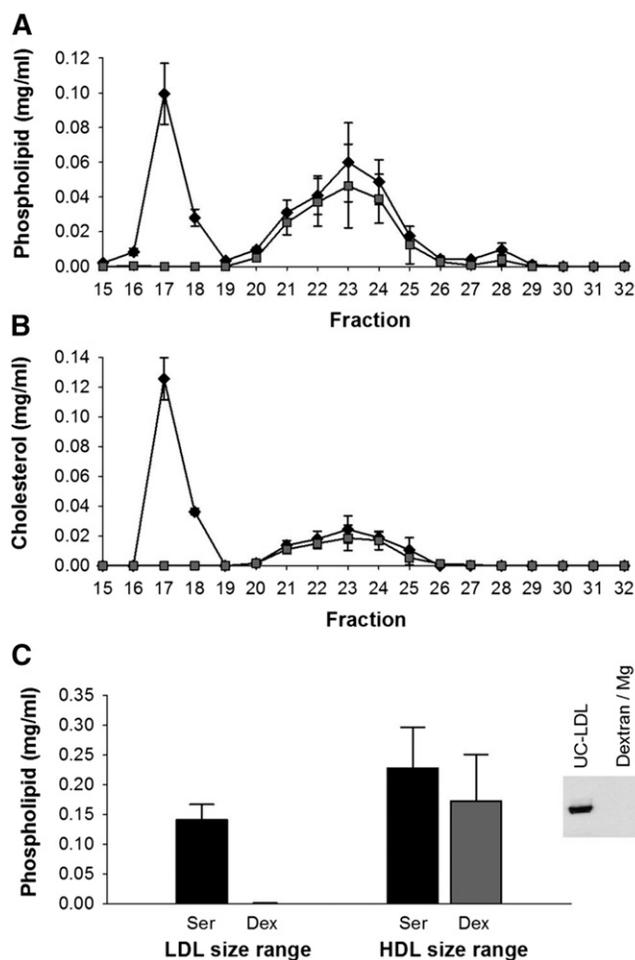


Fig. 2. Phospholipid and cholesterol distribution across lipoprotein subspecies separated by gel filtration chromatography before and after apoB depletion of serum by dextran sulfate/MgCl₂. Data are mean and SD (*n* = 3). Serum control versus apoB depletion using dextran sulfate/MgCl₂. All samples were diluted with STB to equal volume prior to gel filtration chromatography. Phospholipid distribution (A), cholesterol distribution (B), and AUC of LDL and HDL fractions in serum versus apoB-depleted serum (C). The inset in (C) is a Western blot detection of apoB before and after serum apoB depletion with dextran sulfate/MgCl₂. Serum control (black diamond); dextran sulfate/MgCl₂ apoB-depleted serum (gray square).

size (Fig. 1A, B). However, the AUC of phospholipid for the HDL-sized particles did not change significantly (Fig. 1C).

Dextran sulfate/MgCl₂ treatment compared with serum also showed a quantitative depletion of VLDL/LDL phospholipid, cholesterol, and apoB (Fig. 2A–C). In this case, the peak in the HDL size range did not shift toward smaller particles as it did for PEG. However, there was a trend toward a lower AUC for phospholipid in the HDL size range after apoB depletion, *P* = 0.050.

Heparin sodium/MnCl₂ exhibited the least impact on lipid content of particles in the HDL size range (Fig. 3A–C). Phospholipid and cholesterol in the HDL size range were superimposed on that of the control serum, even after removal of the VLDL/LDL. LipoSep IP also quantitatively depleted VLDL/LDL of phospholipid, cholesterol, and

apoB (Fig. 4A–C), with the peak of phospholipid and cholesterol shifted by one fraction.

Protein distributions

apoA-I. apoA-I distribution was evaluated by Western blotting across the HDL size range after the various precipitation strategies. Figure 5A shows that the apoA-I distribution in the HDL size range was shifted to the right after the PEG treatment, mirroring the phospholipid and cholesterol changes. The apoA-I distribution tracked with the phospholipid for both dextran sulfate/MgCl₂ and with heparin sodium/MnCl₂ and did not change the overall pattern or levels of apoA-I (Fig. 5B, C). LipoSep IP resulted in lower levels of apoA-I across the HDL size range.

apoE. Given that large HDL particles are known to be enriched in apoE, we assessed the impact of the various apoB depletion methods on apoE in the HDL size range.

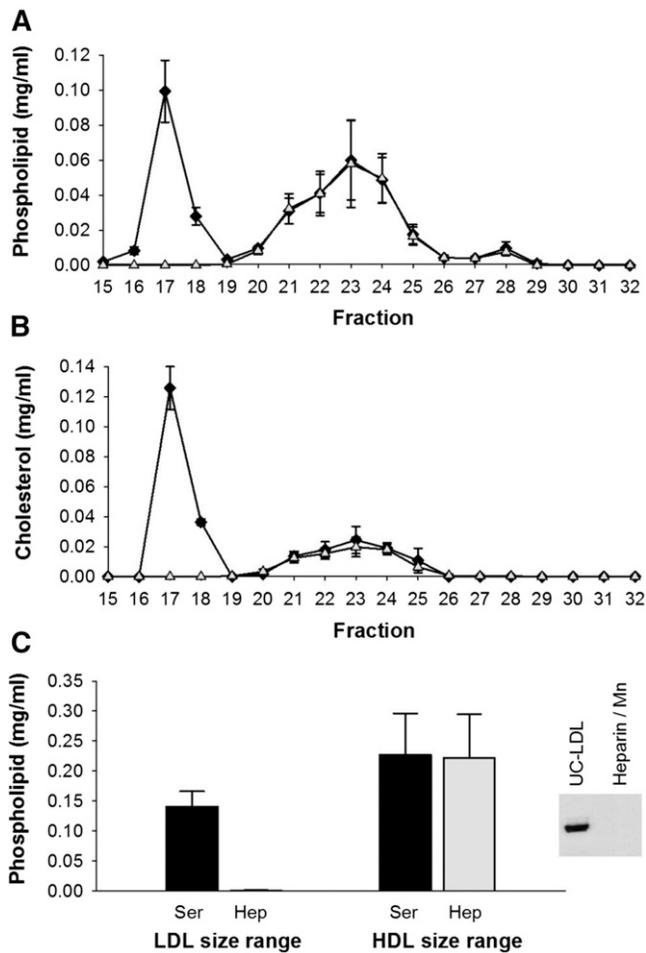


Fig. 3. Phospholipid and cholesterol distribution across lipoprotein subspecies separated by gel filtration chromatography before and after apoB depletion of serum by heparin sodium/MnCl₂. Data are mean and SD (*n* = 3). Serum control versus apoB depletion using heparin sodium/MnCl₂. All samples were diluted with STB to equal volume prior to gel filtration chromatography. Phospholipid distribution (A), cholesterol distribution (B), and AUC of LDL and HDL fractions in serum versus apoB-depleted serum (C). The inset in (C) is Western blot detection of apoB before and after serum apoB depletion with heparin sodium/MnCl₂. Serum control (black diamond); heparin sodium/MnCl₂ apoB-depleted serum (open triangle).

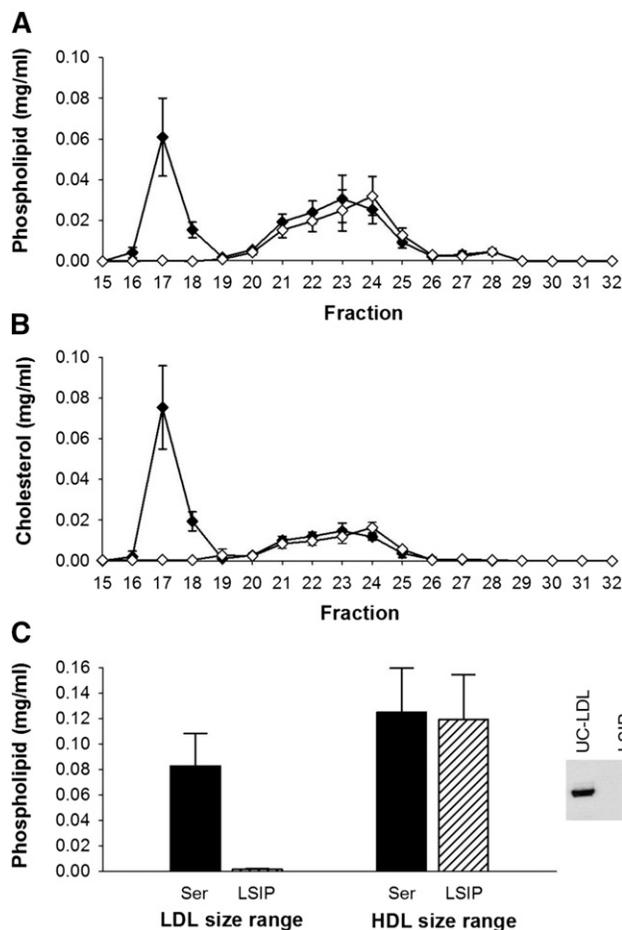


Fig. 4. Phospholipid and cholesterol distribution across lipoprotein subspecies separated by gel filtration chromatography before and after apoB depletion of serum by LipoSep IP. Data are mean and SD (*n* = 3). Serum control versus apoB depletion using LipoSep IP. All samples were diluted with STB to equal volume prior to gel filtration chromatography. Phospholipid distribution (A), cholesterol distribution (B), and AUC of LDL and HDL fractions in serum versus apoB-depleted serum (C). The inset in (C) is Western blot detection of apoB before and after serum apoB depletion with LipoSep IP. Serum control (black diamond); LipoSep IP apoB-depleted serum (open diamond).

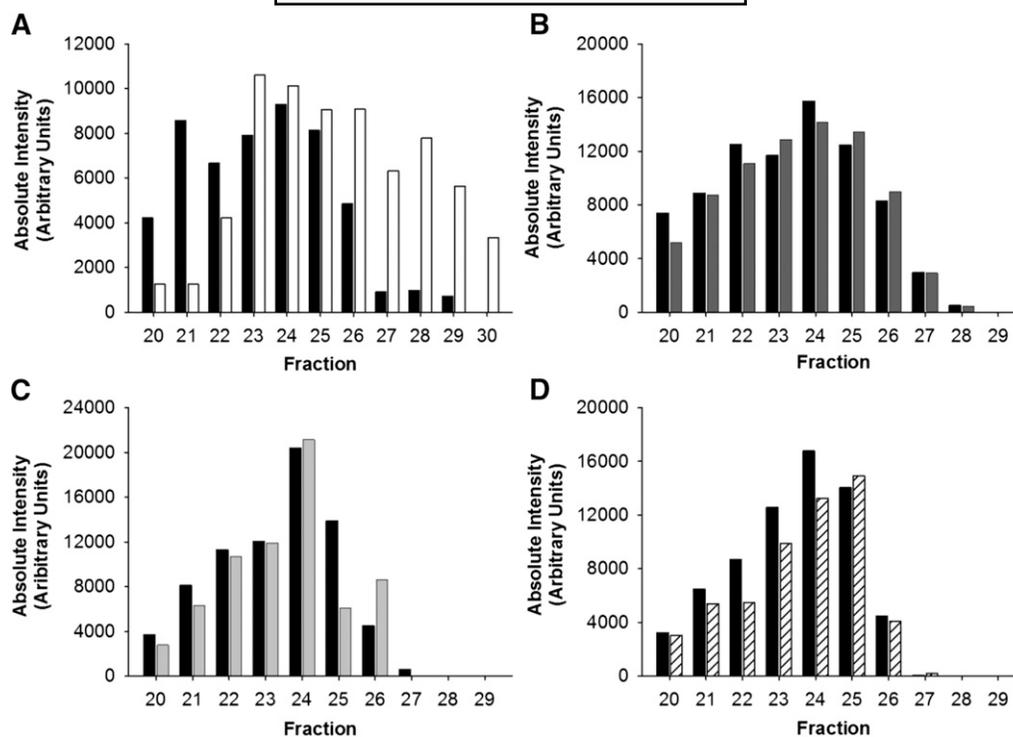


Fig. 5. apoA-I across HDL subspecies before and after apoB depletion. apoA-I levels measured across gel filtration fractions from serum (black bars) compared with apoA-I in fractions after apoB depletion with PEG (white bars) (A), dextran sulfate/MgCl₂ (dark gray bars) (B), heparin sodium/MnCl₂ (light gray bars) (C), and LipoSep IP (diagonal patterned bars) (D). apoA-I was detected via Western blotting. Bands were quantified by densitometry.

The results of a single apoE dot blot are shown in **Fig. 6**. The LipoSep IP experiment was not quantified because of the presence of cross-reacting goat apoE present in the reagent. Unlike for apoA-I, each of the three precipitation methods depleted apoE levels in the larger HDL size range. PEG had the least effect on summed total apoE levels across the HDL range, but consistent with our previous analyses, there was a clear rightward shift with smaller HDL-sized particles exhibiting increased levels of apoE versus control. Dextran sulfate/MgCl₂ and heparin sodium/MnCl₂ methods significantly reduced apoE levels in the fractions containing larger particles with differences of -33 and -50% , respectively, in fraction 20. Fractions containing smaller particles were less affected by dextran sulfate/MgCl₂ and heparin sodium/MnCl₂ depletion, and neither precipitation method caused a noticeable shift in overall pattern similar to PEG apoB depletion.

HDL function

Cholesterol efflux. **Figure 7A** shows the typical pattern of cholesterol efflux from cultured macrophages to each of the HDL-sized lipoprotein fractions from control serum. Most of the cholesterol efflux was promoted by fractions containing medium-sized HDL particles (around fractions 23–24) with less in the fractions containing small HDL particles. When serum was depleted of VLDL/LDL with PEG, there was again a rightward shift of the efflux pattern in the HDL size range, which matched tightly with the shift in phospholipid, cholesterol, and apoA-I observed above

(**Fig. 7A**); however, the total efflux summed across all HDL-sized fractions was not different between the control serum and PEG ($P = 0.773$).

After dextran sulfate/MgCl₂, the efflux to each of the HDL-sized fractions was essentially unchanged from control serum in both magnitude and overall pattern. The total efflux summed across HDL size fractions was also not statistically different ($P = 0.767$, see **Fig. 7B**). Similar results were seen after heparin sodium/MnCl₂ apoB depletion (**Fig. 7C**). Again the summed total efflux across fractions was not different for heparin sodium/MnCl₂ apoB depletion compared with control serum, $P = 0.878$. LipoSep IP reagent showed slightly lower efflux in fraction 21 relative to control serum. However, the summed efflux across the HDL size range was not different from the control, $P = 0.582$ (**Fig. 7D**).

HDL anti-oxidation. **Figure 8A** shows a typical functional readout resulting from HDL-sized particles in serum. There were two peaks of anti-oxidation activity (noted by a decrease in the propagation rate). One was centered on fraction 23, where the largest amount of HDL phospholipid and apoA-I was located. A second peak appeared at fraction 28 in small and poorly lipidated species. PEG apoB-depleted serum (**Fig. 8A**) showed a loss of the peak in the large HDL size range (fraction 22, $P < 0.01$ compared with control serum). Additionally, the antioxidant activity persisted much later in the gradient in the presence of PEG compared with the control (fraction 29, $P < 0.01$ compared

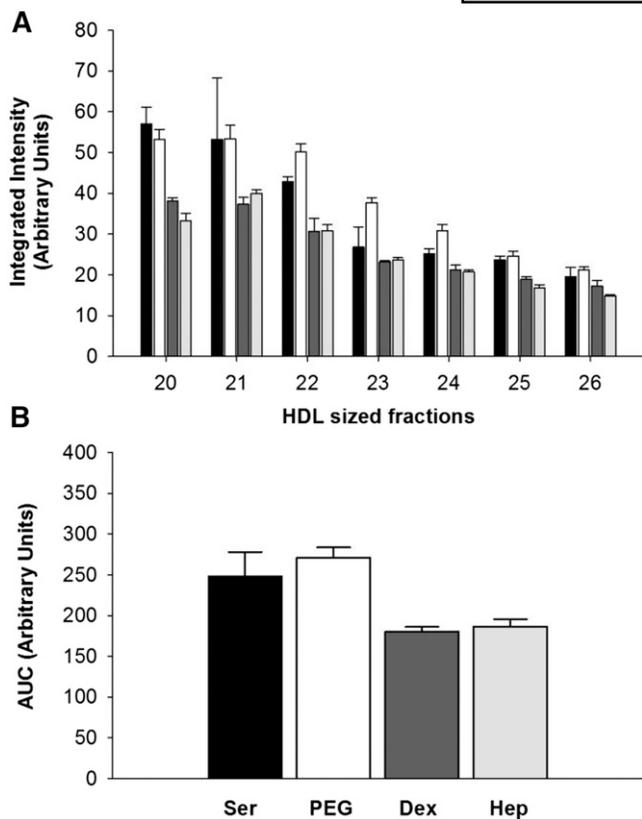


Fig. 6. apoE across HDL subspecies before and after apoB depletion. **A:** apoE in serum (black bars) versus apoE after apoB depletion with PEG (white bars), dextran sulfate/MgCl₂ (dark gray bars), and heparin sodium/MnCl₂ (light gray bars) as determined by a single apoE immunodot blotting. Dots were quantified by densitometry. **B:** AUC of apoE for the HDL-sized fractions.

with serum) consistent with a general shift in the elution pattern. Dextran sulfate/MgCl₂ and heparin sodium/MnCl₂ (Fig. 8B, C) had little effect versus the control on either activity peak. We were unable to obtain interpretable data with the LipoSep IP reagent in this assay, possibly due to the abundant goat proteins in the preparation.

Effects of PEG on HDL particles

Due to the striking differences that we noted with PEG using the gel filtration approach, we further explored the impact of PEG on HDL particle properties. We tested a higher molecular weight PEG (MW 8,000), a shorter incubation of serum for 5 min instead of 20 min with PEG, and a different buffer system with this reagent (glycine buffer instead of water). However, each method recapitulated the rightward shift seen in the data above (not shown). We also sought to determine whether the rightward shift of HDL subspecies upon PEG treatment was related to the process of VLDL/LDL depletion. For this, we took HDL that was isolated by ultracentrifugation (lacking any VLDL/LDL) at roughly the same concentrations found in serum. PEG addition promoted the same rightward shift in the gel filtration elution of HDL measured by both phospholipid and cholesterol as it did in situ in serum (shown in supplementary Fig. 2).

We next quantified the amount of PEG that remained in serum after the VLDL/LDL precipitation. Typically, apoB depletion is performed at 20% (v/v) PEG to plasma volume. To see how much of this comes out of solution with the precipitated LDL and VLDL, we obtained a fluorescein-labeled PEG (MW 6,000; Nanocs, New York, NY) and tracked the reagent in plasma. **Figure 9** compares the total PEG that remained in plasma after a typical VLDL/LDL precipitation reaction with the same amount of labeled PEG in buffer. After separation on the gel filtration system, most of the PEG ran near the total volume of the columns (i.e., the very small range) in both plasma and buffer. Interestingly, the process of VLDL/LDL precipitation only consumed about 20% of the PEG used in the protocol, leaving about 80% (or about 53 mg/ml) behind.

We hypothesized that PEG might interact with the gel filtration column medium to cause an artifactual retention of the HDL particles on the column, thus driving the rightward shift in the profile without a direct effect on HDL particle size per se. We attempted to size the HDL particles in the presence of PEG by several methods that were independent of gel filtration, such as dynamic light scattering and NMR particle sizing. Unfortunately, in each case, the presence of PEG interfered with the analysis, resulting in uninterpretable results (data not shown). We also attempted to remove PEG via dialysis using a membrane with a molecular weight cutoff of 10,000 (Thermo Fisher Scientific). For this experiment, we used fluorescein-labeled PEG. After six 4-liter exchanges with STB, 84.7% of the PEG remained in the sample, demonstrating the impracticality of PEG removal by this method.

However, we were able to analyze these apoB depletion treatments using AF4. This method was chosen because it does not require a separation medium like gel filtration. The phospholipid profile of untreated serum is shown in **Fig. 10**, where the first peak (fractions 3–15) represents HDL-sized particles and the second peak (fractions 25–30) represents VLDL/LDL-sized particles (again, using the presence of apoB as a distinguisher). Upon precipitation with PEG, dextran sulfate/MgCl₂, and heparin sodium/MnCl₂, the VLDL/VLDL peak disappeared consistent with apoB depletion. However, after PEG precipitation, the phospholipid associated with HDL-sized lipoproteins underwent a clear leftward shift compared with unprecipitated serum. Dextran sulfate/MgCl₂ and heparin sodium/MnCl₂ did not shift the peak, though small shoulders appeared in the main HDL peak that could be consistent with some particle rearrangement.

Quantitative MS was performed on the fractions after AF4 separation using isotope-labeled peptide standards for several of HDL's most abundant apolipoproteins. **Figure 11** shows that, in unprecipitated serum, the various apolipoproteins distribute in distinct profiles across the HDL size range. Upon VLDL/LDL precipitation by any method, apoB was quantitatively removed. apoA-I and apoA-II were largely retained after apoB precipitation, but the apoA-I and apoA-II peaks showed a clear leftward shift with PEG that paralleled the lipid profile seen by gel filtration. Dextran sulfate/MgCl₂

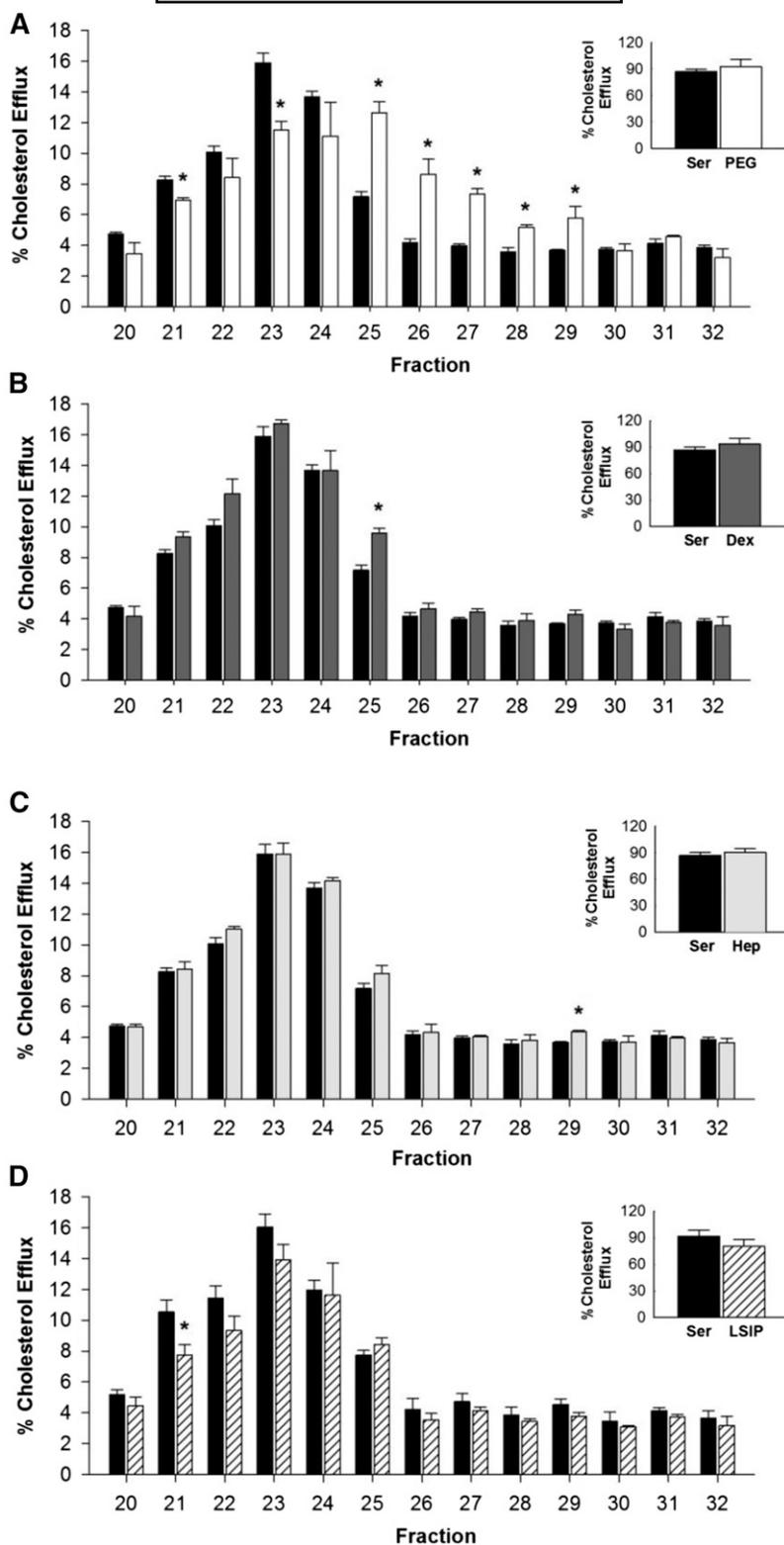


Fig. 7. Cholesterol efflux across lipoprotein subspecies before and after apoB depletion of serum. Data are mean and SD. Each fraction was measured in triplicate. Serum control efflux (black bars) versus apoB depletion efflux with PEG (white bars) (A), dextran sulfate/MgCl₂ (dark gray bars) (B), heparin sodium/MnCl₂ (light gray bars) (C), and LipoSep IP (diagonal line patterned bars) (D). The inset shows the sum of all efflux in the HDL size range. Equal volumes were used across fractions. **P* < 0.01 compared with control serum.

and heparin sodium/MnCl₂ depletion had minimal effects on both apoA-I and apoA-II levels and size. However, we noted distinct changes in other apolipoproteins. Both PEG

and heparin sodium/MnCl₂ depleted levels of apoC-III in the HDL size range, but dextran sulfate/MgCl₂ minimally affected apoC-III. All three precipitation methods

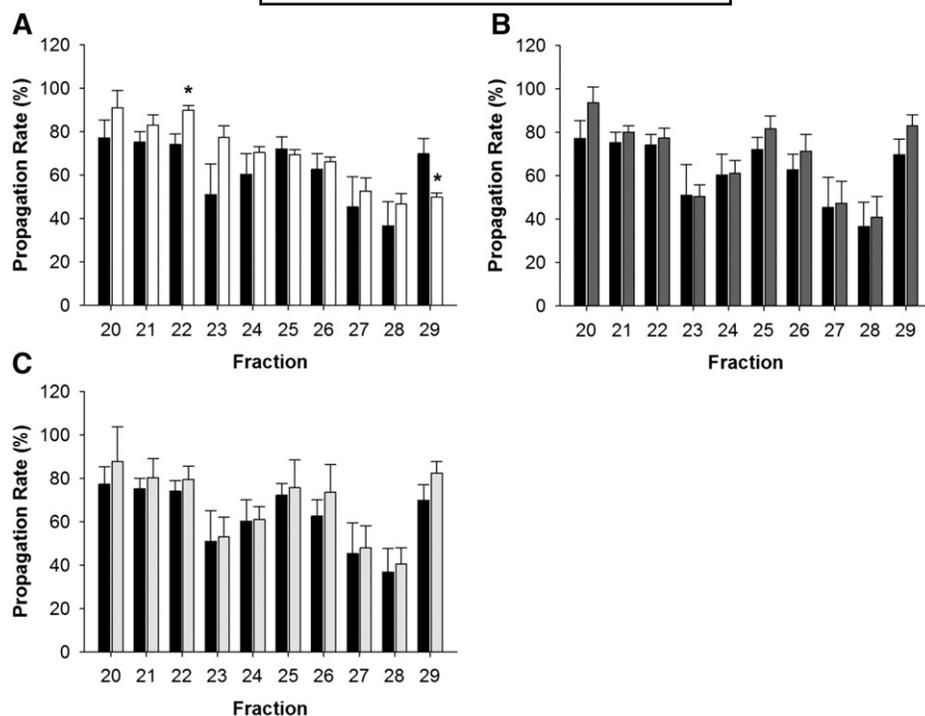


Fig. 8. Ability of HDL to inhibit LDL oxidation across lipoprotein subspecies after apoB depletion of serum. Data are mean and SD. Each fraction was measured in triplicate. Serum control propagation rate (black bars) versus apoB depletion propagation rate with PEG (white bars) (A), dextran sulfate/MgCl₂ (dark gray bars) (B), and heparin sodium/ MnCl₂ (light gray bars) (C). Equal volumes were used across fractions. **P* < 0.01 compared with control serum.

markedly reduced apoE levels, consistent with the gel filtration method. Each of the precipitation methods also affected apoA-IV, apoC-I, and apoC-II in the HDL size range.

We also attempted to use native gel electrophoresis to determine whether HDL size is affected by the presence of PEG. We found that PEG did not affect the apparent diameter of total HDL (isolated by ultracentrifugation) when separated by native PAGE (not shown). However, we also noted that the PEG (as tracked by the fluorescent analog) rapidly separated from the HDL during the gel run, even during the stacking portion of the gel. This indicates that the size-altering effects of PEG are apparent only when present with the HDL particles during the separation (as in the gel filtration and A4F techniques), but once separated from the particles, PEG does not cause these effects.

DISCUSSION

With the realization that HDL function may be more important than HDL-C with regard to CAD risk, many laboratories have initiated large scale efforts to quantify cholesterol efflux in patient serum samples. To reduce variability, the apoB-containing lipoproteins are commonly removed by precipitation to focus primarily on HDL. With recent advances in HDL separation techniques, we sought to assess the impact of the most commonly used apoB precipitation methodologies on the distribution of HDL subspecies and their functions. Our results confirmed

many of the initial characterizations of these methodologies done in the 1980s, including the ability to fully remove VLDL and LDL from human serum/plasma and preserve apoA-I and apoA-II. However, when we probed deeper into the size distribution of the HDL subspecies, we noted some troubling effects. Each apoB depletion method was found to alter HDL in different ways, whether

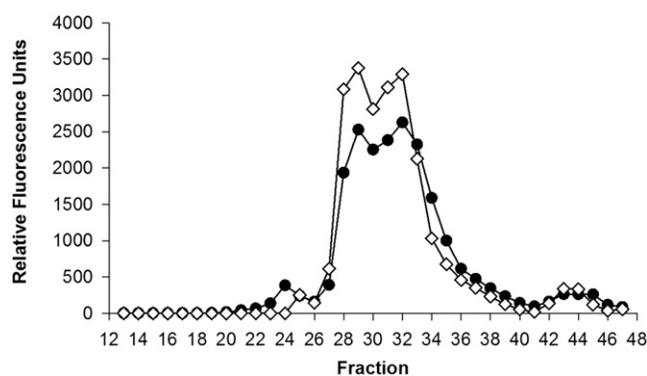


Fig. 9. Fluorescein-PEG (MW 6,000) detection in serum fractions separated by gel filtration chromatography compared with fluorescein-PEG in water. The elution patterns of PEG within an apoB-depleted serum sample (black circles) and in a control buffer (open diamonds) on the triple Superdex Increase column setup were determined by PEG apoB-depleting serum with 20% PEG 6000 containing 1% fluorescein-conjugated PEG (MW 6,000; Nanocs, New York, NY). Fluorescence was measured in each fraction using a BioTek Synergy HT plate reader at excitation and emission wavelengths of 495 and 520 nm, respectively.

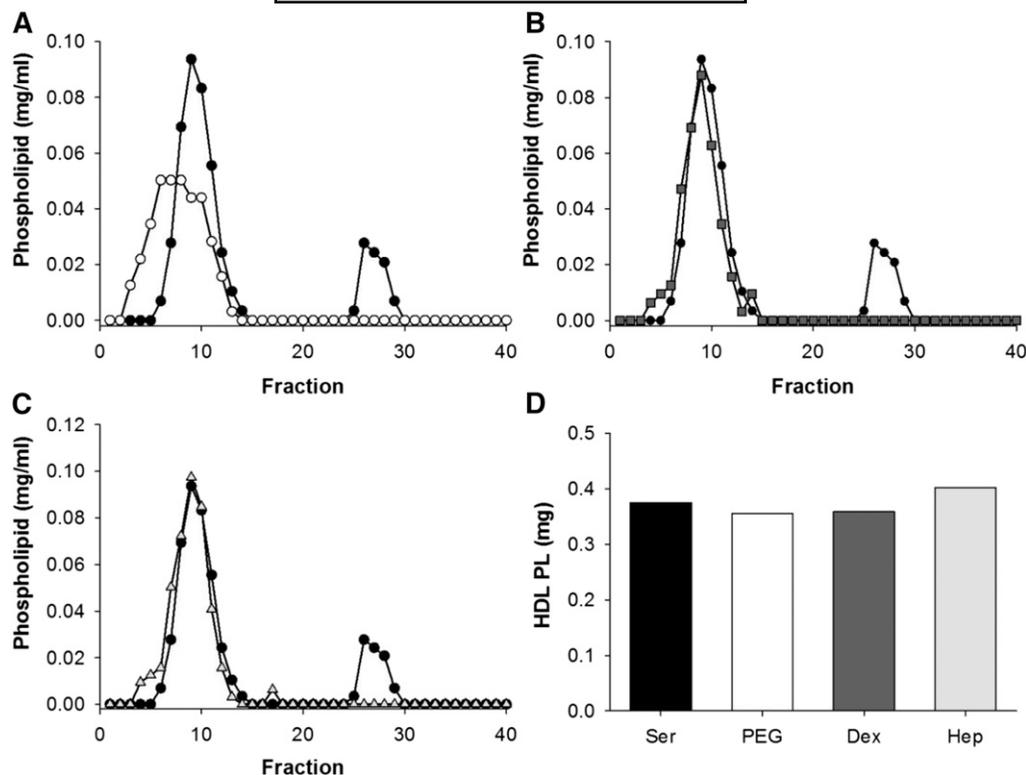


Fig. 10. Phospholipid distribution across lipoprotein subspecies as separated by AF4 before and after PEG apoB depletion of serum. Lipoproteins were separated by AF4. Serum control (black circles) versus apoB depletion with PEG (open circles) (A), dextran sulfate/MgCl₂ (gray squares) (B), and heparin sodium/MnCl₂ (open triangles) (C). D: AUC of phospholipid for HDL fractions in serum (black) versus apoB-depleted serum for PEG (white), dextran sulfate/MgCl₂ (dark gray), heparin sodium/MnCl₂ (light gray). Equal volumes were used.

it was by altering HDL protein content, or changing apparent particle size, or a combination of both. Arguably the most commonly used method, PEG, had profound effects on apparent HDL particle size, while leaving significant amounts of the reagent behind in the sample. First, we will discuss the impact of VLDL/LDL precipitation on HDL subpopulations and then comment on the overall implications on HDL functional analyses.

The profound rightward shift in the HDL elution profile seen with gel filtration after PEG depletion initially suggested that the reagent causes a rearrangement of HDL particles to a smaller size. PEG is a polymer that promotes protein precipitation by steric exclusion. Essentially, proteins are excluded from regions of the solvent occupied by PEG, such that the effective protein concentration increases. Once concentration exceeds the lipoprotein solubility, precipitation occurs. In such a case, it is not difficult to envision a scenario where certain HDL particles might also be affected.

PEG has been shown previously to affect the apparent molecular weight of proteins analyzed by gel filtration. Yan et al. (31) noted that PEG concentrations as low as 5% can cause a shift of protein elution curves to higher elution volume on Sephadex G-75 columns. The magnitude of the effect increased with the size of the protein, with larger proteins having a more pronounced effect than smaller ones. Studies by Atha and Ingham (32) indicated that this does not occur because PEG binds to proteins. Indeed, we

found that PEG separates from HDL when examined by native gel electrophoresis. Furthermore, we were unable to find evidence of strong binding of fluorescent PEG to HDL, despite the fact that we found PEG difficult to remove by dialysis. Thus, PEG must either: 1) affect the resolving power of the gel filtration column media; or 2) modify the hydrodynamic properties of the HDL particles themselves.

The fact that the AF4 technique, which does not rely on a separation medium, showed a similar size reduction of HDL by PEG, strongly supports the latter explanation. The exact effects of PEG on the effective hydrodynamic diameter of HDL particles cannot be determined from these studies, but given the known effects of PEG as an “inert solvent sponge,” we suggest that the residual PEG remaining in solution reduces the hydration shell around HDL particles. This, in turn, alters the size profile of HDL proteins. The reduced hydrodynamic size results in faster diffusion during AF4 and increased partition into the stationary phase of the gel filtration medium. Another way in which PEG could alter HDL particles is by causing the dissociation of certain apolipoproteins, perhaps due to changes in particle hydration. For example, although apoC-III underwent a minor shift to smaller size in Fig. 11, it is clear that PEG treatment also resulted in decreased levels of this protein in the HDL size range. This loss of apolipoprotein content could also account for some of the

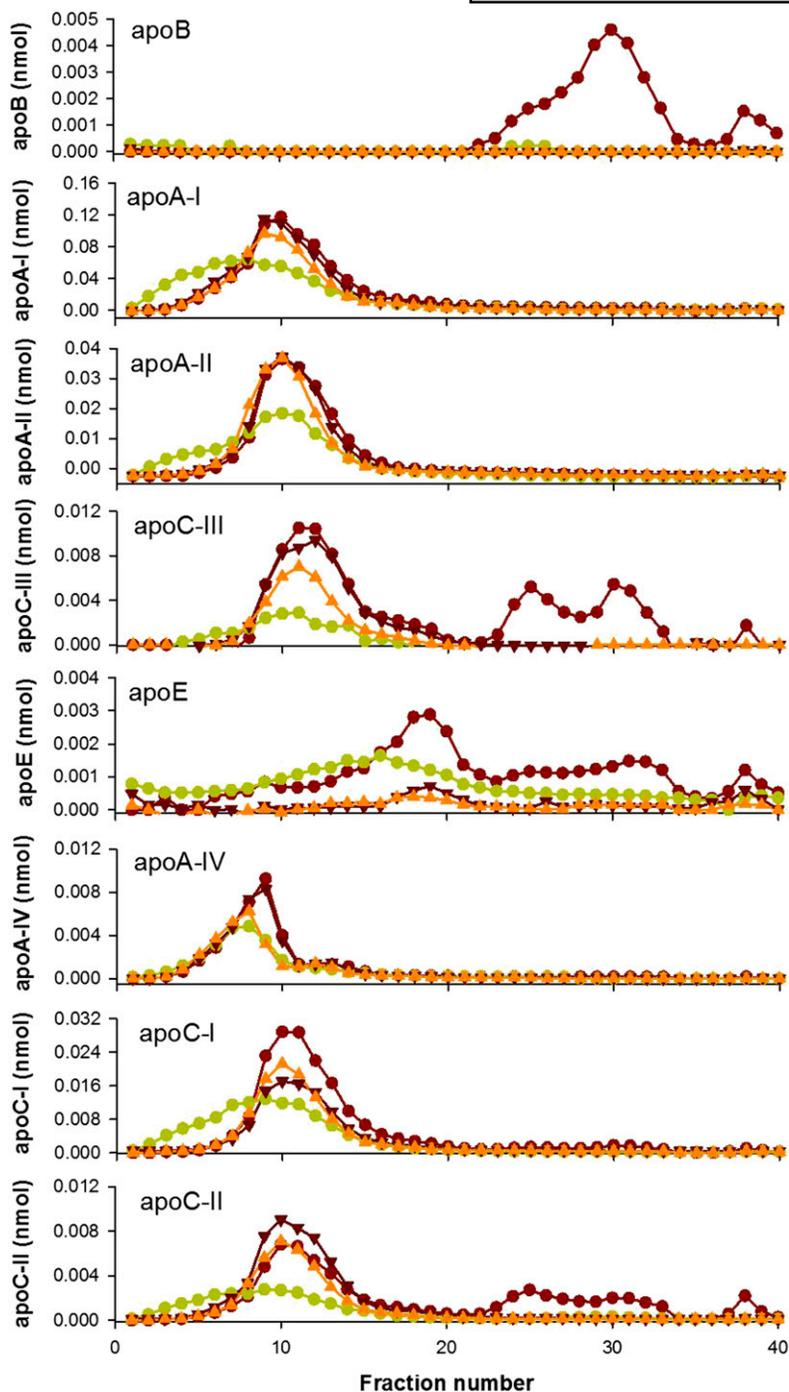


Fig. 11. Quantification of apolipoproteins across lipoprotein subspecies as separated by AF4 before and after apoB depletion. Lipoproteins separated by AF4. Serum control (red circles) versus apoB depletion with PEG (green circles) (A), dextran sulfate/MgCl₂ (dark red inverted triangles) (B), and heparin sodium/MnCl₂ (orange triangles) (C).

size shift to smaller particles. Finally, PEG could cause precipitation of some large HDL particles that are close in size and solubility to LDL.

In contrast, dextran sulfate/MgCl₂ and heparin sodium/MnCl₂ did not affect HDL particle size and both had minimal effects on levels of HDL phospholipid, cholesterol, and apoA-I. Yet, these apoB depletion methods still impacted HDL composition. Both promoted profound reductions in HDL apoE levels (Figs. 6, 11) with less extensive reductions in apoA-IV, apoC-I, and apoC-III. Dextran sulfate/MgCl₂ is known to remove apoE on HDL particles and, in fact, has been previously used to isolate apoE-rich HDL particles (33). The effect of heparin on reduced levels

of apoE and apoC-III is likely explained by their well-known affinity for heparin sulfate proteoglycans (34–36). Heparin is a polyanion that combines with the protein moiety of lipoproteins to form a soluble complex. When the divalent cation, MgCl₂, is introduced, this complex becomes insoluble. Generally, this reaction works best on lipoproteins with a low protein/lipid ratio, like VLDL and LDL. However, given the affinity of apoE and apoC-III to heparin, it is possible that any lipoprotein containing these apolipoproteins is precipitated to some extent. While apoA-IV and the other apoCs are not known to be strong heparin binders, these proteins may associate with either apoE or apoC-III.

Given that each of the above precipitation methods relies on global solubility, it seems that it is nearly impossible to cleanly eliminate one lipoprotein group without affecting the others to some extent. Because the presence of apoB appears to be the best distinguisher between particles with lipid delivery functions (like chylomicrons, VLDL, and LDL) versus those with more diverse functionalities (all the HDL subspecies), an ideal approach would be to immunoprecipitate apoB-containing lipoproteins. We tested one such method, LipoSep IP. While this method, indeed, depleted VLDL and LDL as advertised (37), the reagent contained residual goat proteins in high abundance that complicated further analyses. Additionally, we did note a small but consistent shift in the HDL peak by one fraction which could result from any number of reasons, including adsorption of lipid-free goat apolipoproteins or activity of goat lipid transfer proteins or lipases. Ideally, such a reagent could be purified with immobilized apoB on an easily removable chemical support, though the costs of such a system would likely be high.

Despite the profound effects that PEG had on the size and compositional properties of HDL, the impact of this method on the HDL function was minimal in our hands. Although the cholesterol efflux profile for PEG-depleted serum was shifted to smaller size, the total sum of the HDL fractions to promote cholesterol efflux (i.e., the AUC) did not differ between precipitated and unprecipitated serum. This was surprising given the large residual amount of PEG that remains in the HDL portion of the supernatant. In order to promote cholesterol efflux, HDL particles and lipid-free apolipoproteins must approach the cell surface through an unstirred water layer maintained by the cellular glycocalyx. The presence of PEG in the samples, in addition to decreasing the hydration shell around the HDL particles, might also be expected to impact the unstirred water layer and any number of other cellular processes that could impact cholesterol efflux. Fortunately, these factors do not appear to be critical under the conditions of the cholesterol efflux assays performed here and in other laboratories using similar assays. Indeed, the fact that efflux studies performed with PEG have still managed to reveal important functional differences between normal and CAD individuals attests to this (15, 16, 38). However, the large amount of residual PEG left in solution should give pause when contemplating functional assays in the future, particularly those that rely on interactions that could be perturbed by changes in lipoprotein solubility.

As with cholesterol efflux, none of the precipitation methods exhibited significant deleterious effects on the ability of the HDL fractions to protect LDL from oxidation. This suggests that the compositional or physical property requirements for this function are not perturbed by the methodologies. However, the possibility remains that the residual PEG in solution might pose a problem as novel HDL bioassays are developed. For example, if one were interested in the ability of serum HDL to prevent LDL from binding to heparin sulfate proteoglycans, all of these methods could be envisioned to provide misleading results due to their depletion of apoE in the HDL range.

In conclusion, we noted changes in HDL size profile or composition using each of the tested apoB precipitation methods. Given the fact that the dextran sulfate/MgCl₂ and heparin sodium/MnCl₂ methods did not have the effects on HDL apparent size and also did not impact the AUC of the cholesterol efflux, we propose that these methods may be a better choice for standardized cholesterol efflux assays performed in the future. However, the impact of any chosen apoB precipitation method on HDL composition and size should be carefully examined when bringing new functional study assays online related to endothelial function, inflammation, innate immune function, and others. ■■

REFERENCES

1. Castelli, W. P., R. J. Garrison, P. W. Wilson, R. D. Abbott, S. Kalousdian, and W. B. Kannel. 1986. Incidence of coronary heart disease and lipoprotein cholesterol levels. The Framingham Study. *JAMA*. **256**: 2835–2838.
2. deGoma, E. M., N. J. Leeper, and P. A. Heidenreich. 2008. Clinical significance of high-density lipoprotein cholesterol in patients with low low-density lipoprotein cholesterol. *J. Am. Coll. Cardiol.* **51**: 49–55.
3. Barter, P. J., M. Caulfield, M. Eriksson, S. M. Grundy, J. J. Kastelein, M. Komajda, J. Lopez-Sendon, L. Mosca, J. C. Tardif, D. D. Waters, et al. 2007. Effects of torcetrapib in patients at high risk for coronary events. *N. Engl. J. Med.* **357**: 2109–2122.
4. Bots, M. L., F. L. Visseren, G. W. Evans, W. A. Riley, J. H. Revkin, C. H. Tegeler, C. L. Shear, W. T. Duggan, R. M. Vicari, D. E. Grobbee, et al. 2007. Torcetrapib and carotid intima-media thickness in mixed dyslipidaemia (RADIANCE 2 study): a randomised, double-blind trial. *Lancet*. **370**: 153–160.
5. Schwartz, G. G., A. G. Olsson, M. Abt, C. M. Ballantyne, P. J. Barter, J. Brumm, B. R. Chaitman, I. M. Holme, D. Kallend, L. A. Leiter, et al. 2012. Effects of dalcetrapib in patients with a recent acute coronary syndrome. *N. Engl. J. Med.* **367**: 2089–2099.
6. Voight, B. F., G. M. Peloso, M. Orho-Melander, R. Frikke-Schmidt, M. Barbalic, M. K. Jensen, G. Hindy, H. Holm, E. L. Ding, T. Johnson, et al. 2012. Plasma HDL cholesterol and risk of myocardial infarction: a mendelian randomisation study. *Lancet*. **380**: 572–580.
7. Shah, A. S., L. Tan, J. Lu Long, and W. S. Davidson. 2013. The proteomic diversity of high density lipoproteins: our emerging understanding of its importance in lipid transport and beyond. *J. Lipid Res.* **54**: 2575–2585.
8. Salazar, J., L. C. Olivar, E. Ramos, M. Chavez-Castillo, J. Rojas, and V. Bermudez. 2015. Dysfunctional high-density lipoprotein: an innovative target for proteomics and lipidomics. *Cholesterol*. **2015**: 296417.
9. Vaisar, T., S. Pennathur, P. S. Green, S. A. Gharib, A. N. Hoofnagle, M. C. Cheung, J. Byun, S. Vuletic, S. Kassim, P. Singh, et al. 2007. Shotgun proteomics implicates protease inhibition and complement activation in the antiinflammatory properties of HDL. *J. Clin. Invest.* **117**: 746–756.
10. Cuchel, M., and D. J. Rader. 2006. Macrophage reverse cholesterol transport: key to the regression of atherosclerosis? *Circulation*. **113**: 2548–2555.
11. Linsel-Nitschke, P., H. Jansen, Z. Aherrahou, S. Belz, B. Mayer, W. Lieb, F. Huber, W. Kremer, H. R. Kalbitzer, J. Erdmann, et al. 2009. Macrophage cholesterol efflux correlates with lipoprotein subclass distribution and risk of obstructive coronary artery disease in patients undergoing coronary angiography. *Lipids Health Dis.* **8**: 14.
12. Mehta, N. N., R. Li, P. Krishnamoorthy, Y. Yu, W. Farver, A. Rodrigues, A. Raper, M. Wilcox, A. Baer, S. DerOhannessian, et al. 2012. Abnormal lipoprotein particles and cholesterol efflux capacity in patients with psoriasis. *Atherosclerosis*. **224**: 218–221.
13. Roe, A., J. Hillman, S. Butts, M. Smith, D. Rader, M. Playford, N. N. Mehta, and A. Dokras. 2014. Decreased cholesterol efflux capacity and atherogenic lipid profile in young women with PCOS. *J. Clin. Endocrinol. Metab.* **99**: E841–E847.

14. Kunitake, S. T., and J. P. Kane. 1982. Factors affecting the integrity of high density lipoproteins in the ultracentrifuge. *J. Lipid Res.* **23**: 936–940.
15. Khera, A. V., M. Cuchel, M. de la Llera-Moya, A. Rodrigues, M. F. Burke, K. Jafri, B. C. French, J. A. Phillips, M. L. Mucksavage, R. L. Wilensky, et al. 2011. Cholesterol efflux capacity, high-density lipoprotein function, and atherosclerosis. *N. Engl. J. Med.* **364**: 127–135.
16. Rohatgi, A., A. Khera, J. D. Berry, E. G. Givens, C. R. Ayers, K. E. Wedin, I. J. Neeland, I. S. Yuhanna, D. R. Rader, J. A. de Lemos, et al. 2014. HDL cholesterol efflux capacity and incident cardiovascular events. *N. Engl. J. Med.* **371**: 2383–2393.
17. Rohatgi, A. 2015. High-density lipoprotein function measurement in human studies: focus on cholesterol efflux capacity. *Prog. Cardiovasc. Dis.* **58**: 32–40.
18. Iverius, P. H., and T. C. Laurent. 1967. Precipitation of some plasma proteins by the addition of dextran or polyethylene glycol. *Biochim. Biophys. Acta.* **133**: 371–373.
19. Kimberly, M. M., E. T. Leary, T. G. Cole, and P. P. Waymack. 1999. Selection, validation, standardization, and performance of a designated comparison method for HDL-cholesterol for use in the cholesterol reference method laboratory network. *Clin. Chem.* **45**: 1803–1812.
20. Puchois, P., C. Luley, and P. Alaupovic. 1987. Comparison of four procedures for separating apolipoprotein A- and apolipoprotein B-containing lipoproteins in plasma. *Clin. Chem.* **33**: 1597–1602.
21. Warnick, G. R., T. Nguyen, and A. A. Albers. 1985. Comparison of improved precipitation methods for quantification of high-density lipoprotein cholesterol. *Clin. Chem.* **31**: 217–222.
22. Rached, F., R. D. Santos, L. Camont, M. H. Miname, M. Lhomme, C. Dauteuille, S. Lecocq, C. V. Serrano, Jr., M. J. Chapman, and A. Kontush. 2014. Defective functionality of HDL particles in familial apoA-I deficiency: relevance of alterations in HDL lipidome and proteome. *J. Lipid Res.* **55**: 2509–2520.
23. Gordon, S. M., J. Deng, L. J. Lu, and W. S. Davidson. 2010. Proteomic characterization of human plasma high density lipoprotein fractionated by gel filtration chromatography. *J. Proteome Res.* **9**: 5239–5249.
24. Toth, P. P., P. J. Barter, R. S. Rosenson, W. E. Boden, M. J. Chapman, M. Cuchel, R. B. D'Agostino, Sr., M. H. Davidson, W. S. Davidson, J. W. Heinecke, et al. 2013. High-density lipoproteins: a consensus statement from the National Lipid Association. *J. Clin. Lipidol.* **7**: 484–525.
25. Umaerus, M., B. Rosengren, B. Fagerberg, E. Hurt-Camejo, and G. Camejo. 2012. HDL2 interferes with LDL association with arterial proteoglycans: a possible athero-protective effect. *Atherosclerosis.* **225**: 115–120.
26. Burstein, M., A. Fine, V. Atger, E. Wirbel, and A. Girard-Globa. 1989. Rapid method for the isolation of two purified subfractions of high density lipoproteins by differential dextran sulfate-magnesium chloride precipitation. *Biochimie.* **71**: 741–746.
27. Warnick, G. R., and J. J. Albers. 1978. A comprehensive evaluation of the heparin-manganese precipitation procedure for estimating high density lipoprotein cholesterol. *J. Lipid Res.* **19**: 65–76.
28. Adorni, M. P., F. Zimetti, J. T. Billheimer, N. Wang, D. J. Rader, M. C. Phillips, and G. H. Rothblat. 2007. The roles of different pathways in the release of cholesterol from macrophages. *J. Lipid Res.* **48**: 2453–2462.
29. Yancey, P. G., A. E. Bortnick, G. Kellner-Weibel, M. de la Llera-Moya, M. C. Phillips, and G. H. Rothblat. 2003. Importance of different pathways of cellular cholesterol efflux. *Arterioscler. Thromb. Vasc. Biol.* **23**: 712–719.
30. Kontush, A., S. Chantepie, and M. J. Chapman. 2003. Small, dense HDL particles exert potent protection of atherogenic LDL against oxidative stress. *Arterioscler. Thromb. Vasc. Biol.* **23**: 1881–1888.
31. Yan, S. B., D. A. Tuason, V. B. Tuason, and W. H. Frey 2nd. 1984. Polyethylene glycol interferes with protein molecular weight determinations by gel filtration. *Anal. Biochem.* **138**: 137–140.
32. Atha, D. H., and K. C. Ingham. 1981. Mechanism of precipitation of proteins by polyethylene glycols. Analysis in terms of excluded volume. *J. Biol. Chem.* **256**: 12108–12117.
33. Chiba, H., K. Akizawa, S. Fujisawa, T. Osaka-Nakamori, N. Iwasaki, H. Suzuki, S. Intoh, K. Matsuno, T. Mitamura, and K. Kobayashi. 1992. A rapid and simple quantification of human apolipoprotein E-rich high-density lipoproteins in serum. *Biochem. Med. Metab. Biol.* **47**: 31–37.
34. Futamura, M., P. Dhanasekaran, T. Handa, M. C. Phillips, S. Lund-Katz, and H. Saito. 2005. Two-step mechanism of binding of apolipoprotein E to heparin: implications for the kinetics of apolipoprotein E-heparan sulfate proteoglycan complex formation on cell surfaces. *J. Biol. Chem.* **280**: 5414–5422.
35. Olin-Lewis, K., J. L. Benton, J. C. Rutledge, D. G. Baskin, T. N. Wight, and A. Chait. 2002. Apolipoprotein E mediates the retention of high-density lipoproteins by mouse carotid arteries and cultured arterial smooth muscle cell extracellular matrices. *Circ. Res.* **90**: 1333–1339.
36. Olin-Lewis, K., R. M. Krauss, M. La Belle, P. J. Blanche, P. H. Barrett, T. N. Wight, and A. Chait. 2002. ApoC-III content of apoB-containing lipoproteins is associated with binding to the vascular proteoglycan biglycan. *J. Lipid Res.* **43**: 1969–1977.
37. Contois, J. H., A. L. Albert, and R. A. Nguyen. 2014. Immunoprecipitation of apolipoprotein B-containing lipoproteins for isolation of HDL particles. *Clin. Chim. Acta.* **436**: 348–350.
38. Li, X. M., W. H. Tang, M. K. Mosior, Y. Huang, Y. Wu, W. Matter, V. Gao, D. Schmitt, J. A. Didonato, E. A. Fisher, et al. 2013. Paradoxical association of enhanced cholesterol efflux with increased incident cardiovascular risks. *Arterioscler. Thromb. Vasc. Biol.* **33**: 1696–1705.